

# Electrical conductivity and dehydration steps of gel-grown $\text{CdC}_2\text{O}_4 \cdot 3\text{H}_2\text{O}$

S. K. ARORA, TOMY ABRAHAM, R. S. GODBOLE,

D. LAKSHMINARAYANA

*Department of Physics, Sardar Patel University, Vallabh Vidyanagar 388 120, Gujarat, India*

Electrical conductivity measurement (d.c.), dynamic TGA and DSC analysis of  $\text{CdC}_2\text{O}_4 \cdot 3\text{H}_2\text{O}$  in single crystalline and polycrystalline pellet forms have been carried out in the temperature range 25 to 350° C. Though the dehydration begins at 72° C there is no strict consistency observed in the three dehydration temperatures in different forms of the sample with different contacts. The DSC study reveals the dependence of peak temperature on heating rate. The observed dehydration peaks are believed to be due to the dehydration of the crystal on heating and dissociation of a fraction of the released water molecules.

## 1. Introduction

Study of electrical conductivity of hydrated solids is usefully made for the determination of the number of water molecules present in the crystal structure and their steps of dehydration [1-3]. Cadmium oxalate trihydrate crystals, to the authors' knowledge, have not been subjected to dehydration studies. The purpose of this paper is to investigate the role of the water molecules which escape on heating, in the conduction mechanism. The study of electrical conduction in conjunction with the thermal behaviour has been used to understand the mechanism of conduction in hydrated cadmium oxalate crystals.

## 2. Experimental procedure

### 2.1. Specimen preparation

Single crystals of cadmium oxalate were grown by the gel technique, described elsewhere [4]. From the batch, well-developed and transparent crystals of 8 mm × 5 mm × 5 mm size were selected. With these crystals, bounded by over a dozen habit faces, it was not possible to determine accurately their specific areas. To minimize the inconvenience and error, a crystal was cleaved along the only cleavage plane, (110), twice, such that a thin central slab with parallelepiped geometry could be used for the desired electrical measurements. Pel-

lets of 0.75 cm diameter and 0.2 to 0.4 cm thickness were also prepared at a pressure of  $235 \times 10^3 \text{ Nm}^{-3}$  using a hand-operated hydraulic press and a suitable die.

### 2.2. Electrical conductivity measurements

A porcelain conductivity cell, specially designed for the investigation, is shown schematically in Fig. 1. The crystal or pellet, as the case may be, was mounted between the flat platinum electrodes. To insure perfect contact silver paint was applied on the specimen faces. Experiments were also performed without the application of silver paint on samples. A Pt/Pt-Rh13% thermocouple was connected to the lower electrode for monitoring the specimen temperature. The thermocouple wires served as connecting leads. The conductivity cell was enclosed in a resistance-heated furnace and the temperature of the sample increased by regulating the input power. The rate of heating could be maintained linear for a reasonably large range of temperature.

## 3. Observations and results

The d.c. conductivity,  $\sigma$ , at different temperatures was determined for pellets as well as single crystalline samples, with and without silver paint applied on their faces and some of the results are sum-

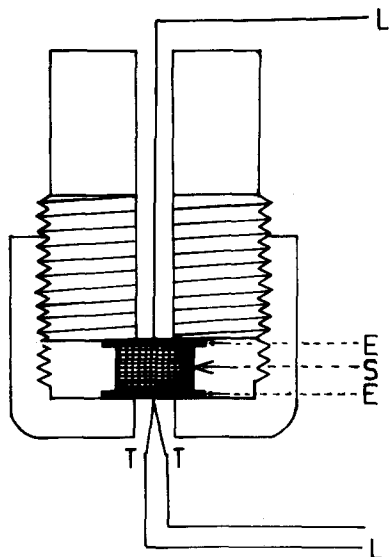


Figure 1 Schematic diagram of the conductivity cell. L, connecting leads; E, platinum electrodes; S, sample; T, thermocouple leads.

marized in Table I. The variation of  $\ln \sigma$  with temperature of silvered and nonsilvered pellets is depicted in Figs. 2a and b. It turns out that in the case of silvered pellet (Fig. 2a) a continuous, sharp drop of conductivity occurs from  $3.942 \times 10^{-10} \text{ ohm}^{-1} \text{ cm}^{-1}$  at room temperature ( $36^\circ \text{C}$ ) to  $1.261 \times 10^{-12} \text{ ohm}^{-1} \text{ cm}^{-1}$  at  $72^\circ \text{C}$ , beyond which the conductivity increases rapidly by about 11 in

the  $\ln \sigma$  scale. This prominent maximum obtained at  $78^\circ \text{C}$  can be recognized as the first dehydration peak, although the first water molecule has already begun to loosen from the lattice at  $72^\circ \text{C}$ . The conductivity does not seem to vary appreciably before the commencement of the second peak, corresponding to the escape of the second  $\text{H}_2\text{O}$  molecule at  $87^\circ \text{C}$ . The second peak is not so apparent on the  $\ln \sigma$  against  $T$  plot, but is quite obvious from the current against time data. From the second peak is seen emerging the third dehydration peak at  $92.5^\circ \text{C}$ . The current then drops monotonically after the third dehydration peak, the conductivity drop being of the order of 14 in the  $\ln \sigma$  scale. The decrease is quite short-lived, as it is evident from Fig. 2a that at about  $122^\circ \text{C}$  the conductivity starts increasing gradually up to a temperature of about  $320^\circ \text{C}$  to acquire a height (on the  $\ln \sigma$  scale) of almost the same value as in the beginning at around  $36^\circ \text{C}$ . Later, with an increase of only  $20^\circ \text{C}$  in temperature, the current in the circuit shoots up to exceed the measurable range.

Interestingly, the sequence with the unsilvered pellet was not found to be exactly identical to that of the silvered one, as is obvious from Fig. 2b. It is seen with the silvered pellet, that initially a definite drop in conduction occurs only up to  $45^\circ \text{C}$  and then a plateau begins extending up to  $72^\circ \text{C}$ . Nevertheless, the electrical transport behaviour at  $72^\circ \text{C}$  and the occurrence of the first dehydration

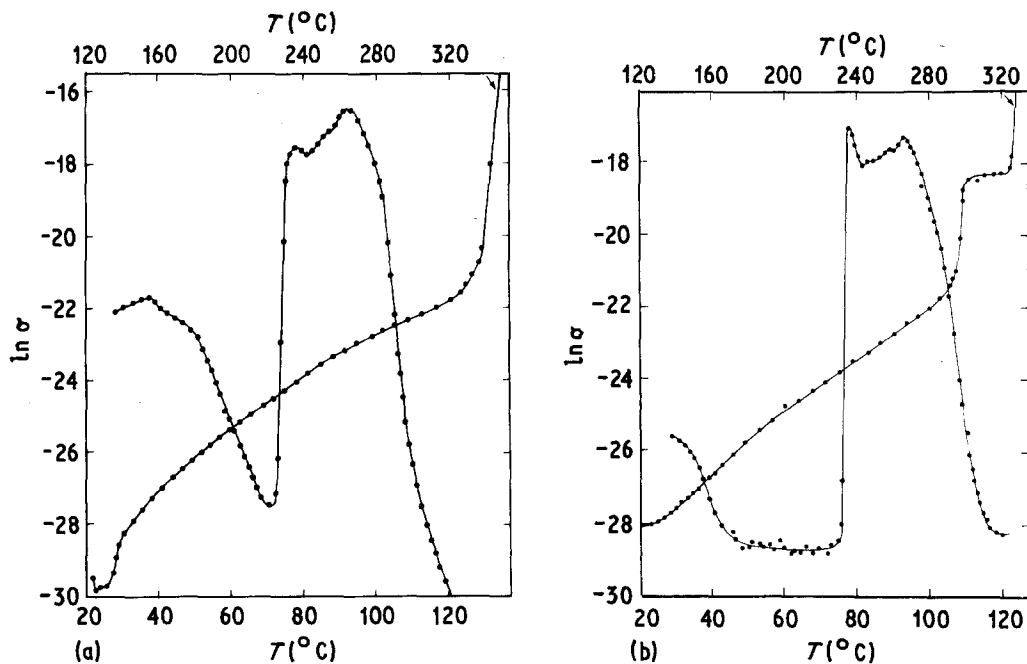


Figure 2 Plot of  $\ln \sigma$  against temperature in the case of (a) silvered pellet and (b) nonsilvered pellet.

TABLE I Observation of electrical parameters of different samples

Sample	First peak			Second peak			Third peak			N (molecules cm <sup>-3</sup> )
	Initiation temperature (°C)	Peak temperature (°C)	$\sigma$ at peak temperature (ohm <sup>-1</sup> cm <sup>-1</sup> )	Initiation temperature (°C)	Peak temperature (°C)	$\sigma$ at peak temperature (ohm <sup>-1</sup> cm <sup>-1</sup> )	Initiation temperature (°C)	Peak temperature (°C)	$\sigma$ at peak temperature (ohm <sup>-1</sup> cm <sup>-1</sup> )	
Silvered pellet	72	78	$2.522 \times 10^{-8}$	82	87	$3.838 \times 10^{-8}$	88	92.5	$7.06 \times 10^{-8}$	$1.601 \times 10^{17}$
Nonsilvered pellet	72	78	$4.38 \times 10^{-8}$	85	89	$2.31 \times 10^{-8}$	90	93	$3.3 \times 10^{-8}$	$1.23 \times 10^{17}$
Silvered crystal	72	80	$3.539 \times 10^{-12}$	—	90	$4.95 \times 10^{-12}$	106	115	$1.708 \times 10^{-11}$	$8.678 \times 10^{13}$
Nonsilvered crystal	Cumulative peak									$1.498 \times 10^{13}$
					128				$4.43 \times 10^{-12}$	

peak at 78° C are exactly identical to those with the silvered pellet (Fig. 2a). A second very feeble peak can be observed at 83° C, the nature of which suggests that it might be a stray peak. Thereafter, a third, small but quite noticeable, peak emerges at 89° C, followed by a fourth one at 93° C.

The heights of the individual peaks in both the cases are, however, not comparable. In the silvered pellet, the first peak at 78° C is shorter by a factor of 1.7 than that of the unsilvered pellet at the same temperature (Figs. 2a and b have been plotted in linear scales in Figs. 4a and b, respectively, which can be conveniently used for visible comparison of peak heights). Secondly, on the silvered pellet, the second peak is less prominent and is seen submerged into the third peak, while in the case of unsilvered pellet, two different intermediate, and slightly spaced peaks are seen emerging between the two extreme peaks. The temperature corresponding to none of these intermediate peaks corresponds to that of the second peak in the silvered pellet. Moreover, the third, and the last dehydration peak in the silvered pellet is a little more prominent than the corresponding peak in the unsilvered pellet, and its height is 2.8 times larger than the first peak. In the case of the unsilvered pellet, on the contrary, the first and the last peaks are of comparable heights, with the last peak shorter than the first one by a factor of 0.7.

The observations in respect of single crystalline samples have been plotted in Fig. 3. The electrical behaviour (in terms of variation of  $\ln \sigma$  with  $T$ ) of silvered crystalline sample (Curve 1) is found to be initially similar to that of the silvered pellet, in that the conductivity decreases noticeably up to 72° C, and then increases slightly to give only one prominent peak. A close observation, however, reveals two jerks at 80° C and 90° C before the current rises to give the prominent peak at 115° C. Later, the conductivity rises from the minimum,  $2.60 \times 10^{-13} \text{ ohm}^{-1} \text{ cm}^{-1}$  at 134° C, following more or less a path similar to that of the pellets. The conductivity of unsilvered crystal (Curve 2) shows, on the average, a general trend to increase with temperature, and there appears one dehydration peak at 128° C. Locating the exact point of the initiation of this peak could, however, not be successfully done because of the steady increase in conductivity in the temperature range studied.

#### 4. Discussion

The observed initial decrease in conductivity with

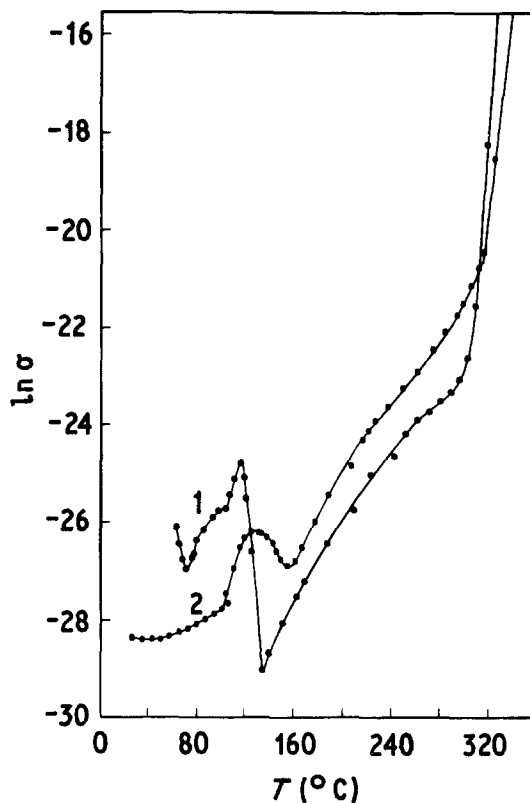


Figure 3 Plot of  $\ln \sigma$  against temperature of silvered (Curve 1) and nonsilvered (Curve 2) crystalline samples.

temperature up to 72° C for the pelletized sample (Fig. 2) may be attributed to the condition of its surface on which are adsorbed some water molecules. The escape of these water molecules from the surface, because of the rising temperature, results in the decrease of conductivity. The effect is similar to that of the individual adsorbed semi-hydrated ions and saturated solution formed by virtue of capillary condensation in grooves on the crystal surface, as observed in NaCl crystal [5, 6]. This initial decrease in conductivity is not so prominent in the case of single crystalline samples (Fig. 3) because the cited adsorption depends upon the particle size. The difference in the behaviour of silvered (Fig. 2a) and non-silvered (Fig. 2b) pellets before commencement of deaquation, i.e., before 72° C, is noteworthy. The higher initial conductivity in the case of the silvered pellet may be attributed to better electrical contact. Evaporation of the surface-adsorbed water molecules finishes around 50 to 65° C in the case of the unsilvered pellet and hence the conductivity remains stable at a minimum level up to the initiation of the first deaquation peak. In the silvered

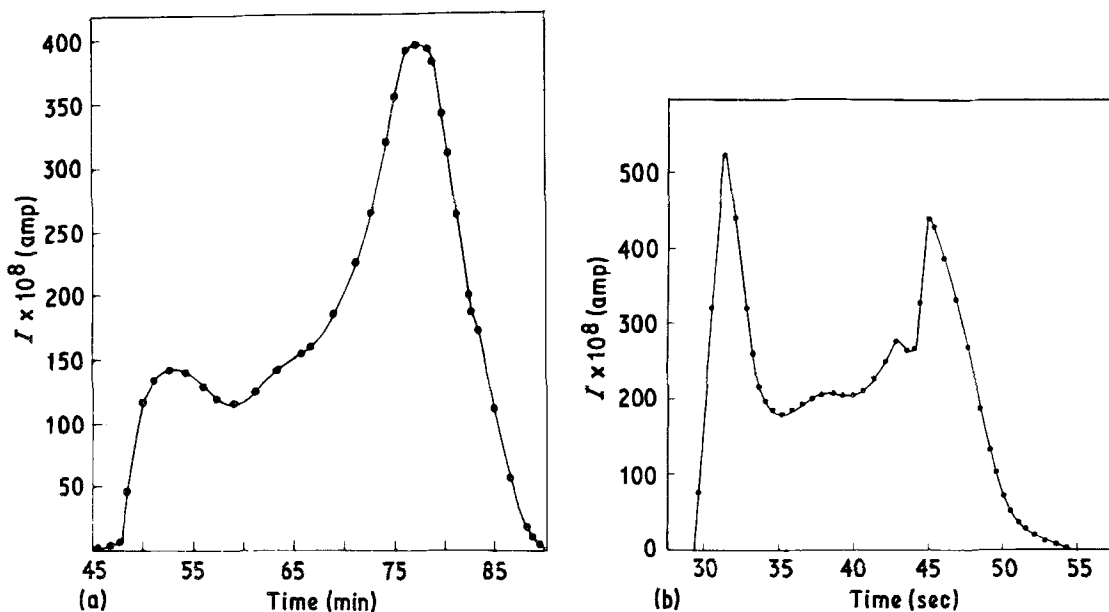


Figure 4 Plot of the variation of current with time for (a) silvered and (b) unsilvered pellets.

pellet, the adsorbed water molecules which are effectively trapped between the surface and the electrodes leave the surface gradually, and hence no plateau region is observed.

Figs. 4a and b and 5a and b represent the plots of current against time for silvered and unsilvered pellets and crystals, respectively. The discrepancy in the peak heights of silvered and nonsilvered pellets could not, however, be accounted for by application of silver paint. Further, the pelletized samples may yield only qualitative results because

of the possibility of significant surface conduction occurring on the extensive internal surface of the pellet [7]. Despite this disadvantage, reproducible data were obtained for the height of the current time peaks, each one of which is a measure of the number of charge carriers involved in the enhanced conduction at the deaquation temperature. An intermediate stray peak in Fig. 4b may be due to trapped water and the dissociated molecules in the interstitials of the pellet which are driven out by the higher temperature and/or the applied field.

It is noteworthy that the combined peak tem-

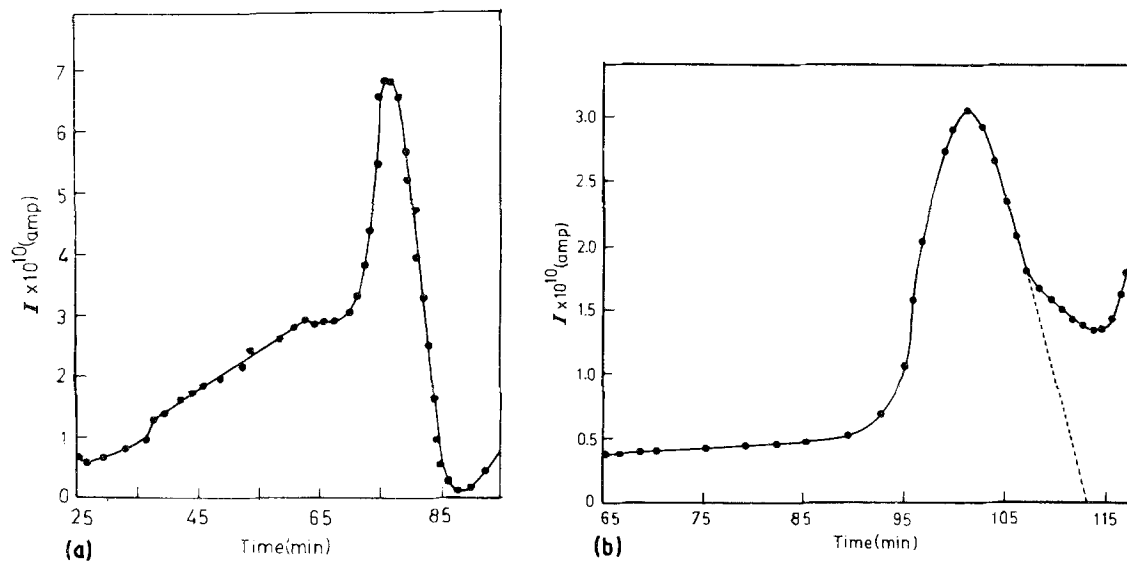


Figure 5 Plot of the variation of current with time for (a) silvered and (b) unsilvered single crystalline samples.

perature, 128° C, (Curve 2 in Fig. 3) coincides with the differential scanning calorimetry (DSC) peak value (Fig. 6a). The observed slight difference in the conductivity values of the two crystalline samples (Fig. 3) may be attributed to the error in dimension measurement. The observed difference in the peak temperature might be due to non-uniform heating rate of different samples. This is also supported from the DSC plots in which the heating rate of 5° C min<sup>-1</sup> resulted (Fig. 6a) in a peak temperature of 128° C, whereas with a heating rate of 10° C min<sup>-1</sup> (Fig. 6b) the peak temperature was elevated to 142° C.

The enormous increase in the conductivity at the dehydration point can be understood as due to a large increase in the concentration of the mobile charge carriers, as suggested by Nandi *et al.* [3] in the similar CuSO<sub>4</sub> · 5H<sub>2</sub>O, if one assumes that the water molecule at 72° C is dissociated into H<sup>+</sup> and OH<sup>-</sup> ions. The total number of charge carriers, *N*, collected in the range of temperature around a peak can be calculated from the current against time curves.

For calculating the number of charge carriers, *N*, which contribute to conduction, separate peaks cannot be taken into account because the current does not come to the ground value before rising to the next peak. Also, since the preceding peak is seen to contribute to the latter one, determination of the extra contribution by a single peak is rather difficult. Hence, a cumulative contribution of all the peaks during the entire dehydration range of temperature is considered to give the required concentration of charged particles and the values thus obtained from Figs. 4a and b and 5a and b are shown in Table I. The higher values of *N* for pellets, compared to crystals, can be qualitatively explained as follows. The ratio of thickness to area (*l/a*) in the case of pellets is a small fraction of that

of crystal samples. The thinner the sample, the easier the collection of the charge carriers by the electrodes. Also the pellets are less dense than the crystal. In the present case, the packing density of pellets is about 89% of the crystals. Therefore, faster diffusion can be achieved in pellets. Moreover, the smaller *l/a* values of pellets is equivalent to larger area in contact with the electrodes as compared to the area exposed to air. Therefore, a larger amount of water vapour coming out of the sample is passed by the sides of the electrodes and hence a greater probability of dissociation is expected. But, crystals on the other hand, having high values of *l/a*, will evaporate their water molecules from the large area of the sample exposed to air, providing comparatively lesser number of water molecules, and hence charged ions, to reach the electrodes. The silver paint contact will block, and hence retain in the sample a part of water vapours from escaping. Larger trapping of the water molecules and better collection of ions by the electrodes may be the plausible reasons for the large number of the mobile charge carriers in the case of silver paste application. Though the conductivity drops to a minimum after the peak, the TGA plot (Fig. 7) shows a continuous decrease in weight with increasing temperature even after the peak. All the water molecules released and dissociated are not able to come out of the sample immediately and many of them are trapped in the interstitial space. These dissociated and trapped H<sup>+</sup> and OH<sup>-</sup> ions are made mobile by the applied field and the increasing temperature. As the temperature crosses the dehydration point, the number of trapped ions decreases at a high rate as they are driven by the applied field and are collected by

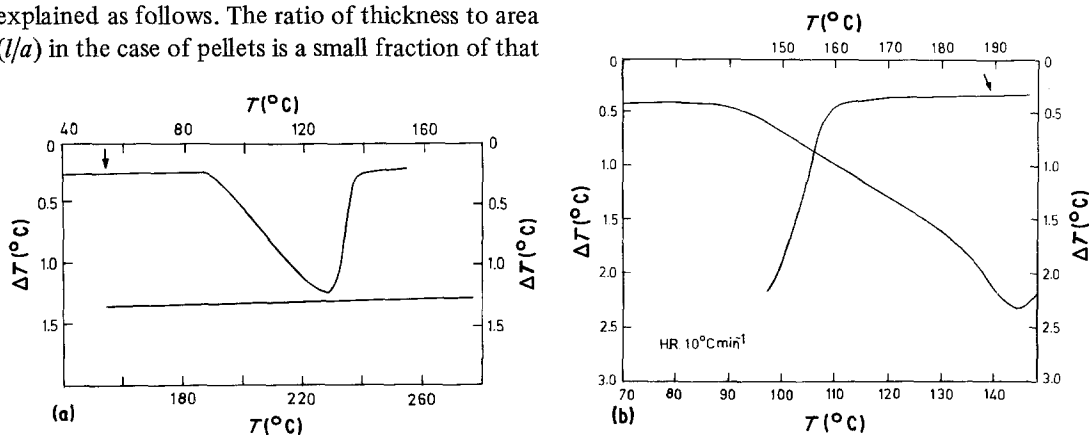


Figure 6 DSC plot of  $\Delta T$  against  $T$ . (a) heating rate  $\simeq 5^\circ \text{C min}^{-1}$ ; (b) heating rate  $\simeq 10^\circ \text{C min}^{-1}$ .

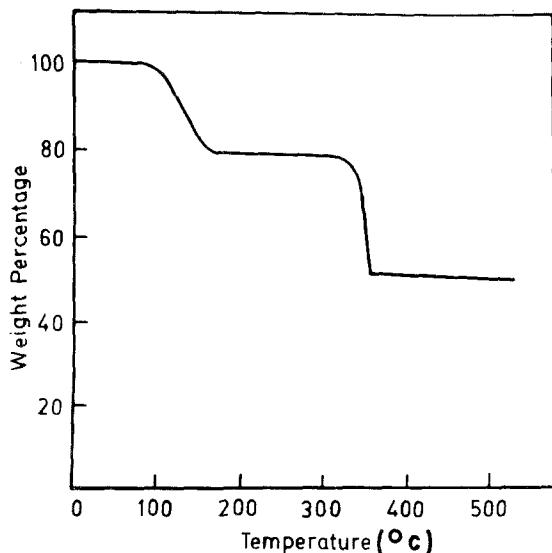


Figure 7 TGA plot of weight percentage against temperature. Initial weight 6.78 mg, heating rate  $10^{\circ}\text{C min}^{-1}$ .

the electrodes. On the other hand, the trapped water molecules can come out slowly by diffusion which is the reason for the typical thermogravimetric analysis (TGA) observation (Fig. 7) showing a reduction in mass for considerable time even after the peak temperature [3].

After the completion of dehydration, all the samples, irrespective of their form or contacts, show a gradual increase in conduction, like any other ionic material, up to around  $300^{\circ}\text{C}$  where the decomposition of the material begins to yield CdO ultimately, evolving  $\text{CO}_2$ . In the presence of atmospheric oxygen the decomposition may be responsible for the enhanced conductivity, due to oxygen deficiency of cadmium oxide formed, in which case the charge carriers are electrons, as observed on other samples [8, 9]. It is inferred from the conductivity data that the final part of the conductivity, after the completion of dehy-

dration, follows an identical path in all the cases of our investigation.

## 5. Conclusions

(1) Dehydration steps of hydrated samples can be investigated by a systematic study of ionic conductivity.

(2) Samples prepared in different ways give different dehydration temperatures, which may be due to the non-uniform and nonlinear heating rates.

(3) Samples with silver paint give a relatively higher number of charge carriers, that calculated for crystalline samples is smaller by approximately 4 orders when compared to pelleted samples.

(4) The possible mechanism responsible for the large increase in current during dehydration is assigned to the ionization of a small fraction of the detached water molecules.

(5) All the samples follow a similar conductivity path after the conclusion of the dehydration process.

## References

1. W. W. WENDLANDT, *Thermo. Chim. Acta* 3 (1970) 171.
2. Z. HALMOS and W. W. WENDLANDT, *ibid* 7 (1973) 95.
3. P. N. NANDI, D. A. DESHPANDE and V. G. KHER, *Proc. Indian Acad. Sci.* 88A (1979) 113.
4. S. K. ARORA and TOMY ABRAHAM, *J. Crystal Growth* 53 (1981) 851.
5. G. SIMKOVICH, *J. Phys. Chem.* 67 (1963) 1002.
6. C. GHEORGHITA and P. CRISTEA, *Bul. Inst. Polytech. Bukuresti* 24 (1962) 43.
7. AH MEE HOR and P. W. M. JACOBS, *J. Solid State Chem.* 22 (1977) 77.
8. P. KOFTAD and A. Z. HED, *J. Amer. Ceram. Soc.* 50 (1967) 681.
9. H. B. LAL and V. PRATAP, *Ind. J. Pure Appl. Phys.* 16 (1978) 519.

Received 20 April

and accepted 24 May 1982